Probing a Nucleon Spin Structure at TESLA by the Real Polarized Gamma Beam

S. Alekhin ^a V. Borodulin ^a

^aInstitute for High Energy Physics, Protvino, Russia

A. Çelikel ^b M. Kantar ^b S. Sultansoy ^{b,1}

^bAnkara University, Dept. of Physics, Ankara, Turkey

Abstract

The recent proposals concerning the usage of the real polarized gamma beam, obtained by the Compton backscattering of the laser photons off the electron beams from either the linear or circular accelerators were considered. The heavy quark photoproduction process giving a unique opportunity to measure polarized gluon distribution was investigated.

Key words: Asymmetry, spin, charm quark, laser, high energy γ -beam

1 Introduction

A spin crisis arose when the first determination of

$$\Delta \Sigma = \Delta u + \Delta d + \Delta s$$

was found to be much smaller than expected [1], where

$$\Delta f \equiv \int dx \Delta f(x, Q^2),$$

and $f(x, Q^2)$ are the polarized quark spin distribution functions. The recent value of the world average for $\Delta\Sigma$ is approximately 0.3 ± 0.06 . It is much

 $[\]overline{\ ^{1}}$ On leave from Institute of Physics, Baku, Azerbaijan

smaller than the relativistic quark model prediction of 0.6 [2]. Among the number of explanations of the EMC results on the longitudinally polarized proton structure function, that of the perturbative QCD approach occupies a prominent position and opens a new domain of tests [3]. It has been shown that in perturbative QCD predictions of the quark-parton model concerning the singlet axial charge contribution to I_1^p need to be modified because of the γ_5 anomaly of the flavour singlet current J_{μ}^5 . In this approach the main question is the size of the polarized gluon distribution. But there is a great uncertainty in theoretical estimates on the magnitude and x-dependence of $\Delta G(x)$, especially in the moderate x-region x > 0.1. One calculation, performed in the framework of MIT Bag Model, predicts negative $\Delta G(x)$ value, thus even sharpening the problem [4].

In order to measure gluon contribution to the nucleon spin, we must select a process where the familiar lowest order graphs of deep inelastic scattering from a single quark are suppressed. Analysis of the experimental data shows that there is no significant charm content in the nucleons [5]. Then one may hope to determine polarized gluon effects in the process of the charmed quark photoproduction. Due to the comparatively large mass of the c-quark the leading mechanism for obtaining a $c\bar{c}$ - pair in the final state is the hard photongluon fusion (PGF) process

$$\gamma + g \to c + \bar{c} \tag{1}$$

and produced $c\bar{c}$ pair may form J/ψ meson or fragment separately into open charm states.

A rich spin physics programme was proposed by COMPASS collaboration at CERN [6]. A large part of it is devoted to measurement of gluon polarization by tagging D^0 , D^{*+} -mesons produced in the γ^*N collisions. Produced D^0 , D^{*+} -mesons will be reconstructed from their two-and three-body decays into hadrons. It permits to impose constraints on the invariant masses of $K \pi \pi$, $K \pi$,.. subsystems, which effectively rejects a background, especially in the case of D^{*+} -tagging. A statistical precision on the polarization asymmetry measurement is expected to be about 0.05.

A proposal has been made [7] to determine $\Delta G(x)$ from the measurement of the asymmetry in the charm photoproduction process in the scattering of polarized real photons off polarized fixed target. In this paper we consider a possibility to realize this experiment at the TESLA machine [8], and discuss briefly an opportunity to perform it at SLAC and LEP2.

2 The Real Gamma Beam

2.1 Linear Accelerator

The scheme of the proposed experiment looks as follows. Circularly polarized laser beam with photon energy $\omega_0 = 3.3 \ eV$ (Cu15 laser) is scattered off the 250 (50) GeV-electrons provided by TESLA (SLAC) [9]. Throughout this subsection the numbers in parentheses refer to the SLAC gamma beam parameters. The Compton back-scattered photon beam has a spectrum $\gamma(y)$

$$\gamma(y) = \frac{1}{N} \times \frac{dN}{dy}, \quad N = \int dy \frac{dN}{dy},$$

$$\frac{dN}{dy} = \frac{1}{1-y} + 1 - y - 4r(1-r),$$
(2)

and follows closely to the trajectory of the primary electron beam. Here the ratio of the hard photon energy ω to the electron energy E_e ranges as

$$y = \frac{\omega}{E_e}, \quad 0 \le y \le y_{max} = \frac{\kappa}{1+\kappa} \sim 0.927 \ (0.717),$$

$$\kappa = \frac{4\omega_0 E_e}{m_e^2} \sim 12.638 \ (2.528), \quad r = \frac{y}{\kappa (1-y)}.$$
(3)

Had the laser beam been circularly polarized, the γ -beam would be polarized too and the γ -beam helicity is given by

$$\xi_2 = \frac{B(y)}{N\gamma(y)},$$

$$B(y) = -\lambda_{ph}(2r-1)\left(\frac{1}{1-y} + 1 - y\right).$$

where λ_{ph} denotes the laser photon helicity. Due to the unique dependence of both γ -beam energy and polarization on the scattering angle θ_{γ} between the incident and scattered photon

$$\theta_{\gamma}(\omega) \sim \frac{m_e}{E_e} \sqrt{\frac{E_e \kappa}{\omega} - (\kappa + 1)},$$

it is possible to obtain almost monochromatic gamma beam with energy $0.99\omega_{max} \leq \omega \leq \omega_{max}$ and polarization nearly equal to unit by selecting photons with $\theta_{\gamma} \leq 0.759 \ (1.93) \cdot 10^{-6} rad$. Taking the distance between the conversion region and collimator 100m, we obtain that this angle corresponds to the diameter of the selecting slit $d = 152 \ (386)\mu m$.

In our further estimation on the luminosity of gamma beam scattering off a polarized fixed target, we shall follow to the method outlined in [10]. We determine the optimal number of converted photons N_{γ} by the requirement to obtain one event per collision

$$\beta N_{\gamma} T_n \sigma_{\gamma p} = 1, \tag{4}$$

where β is the fraction of the photons coming through the slit, T_n stands for the target nucleon density and $\sigma_{\gamma p}$ is the total cross section of gamma-proton collisions. In the case of 1% γ -beam monochromaticity $\beta \sim 4.22~(2.02) \cdot 10^{-2}$, for deuterated butanol target with the length about 40 cm the density is $T_n = 4 \cdot 10^{25} cm^{-2}$ and $\sigma_{\gamma p} \sim 100 \mu b$ at high energies, so we get $N_{\gamma} = 5.92~(12.36) \cdot 10^3$. Because the number of electrons in a bunch $N_e = 5.15~(3.5) \cdot 10^{10}$ for TESLA (SLAC), we obtain the necessary conversion coefficient

$$K = \frac{N_{\gamma}}{N_e} = 1.15 (3.53) \cdot 10^{-7}.$$

The number of photons required to provide the scattering of each electron with the laser photon is defined from

$$\frac{n_0 \sigma_c}{S_{eff}} = 1, (5)$$

where n_0 is the number of photons in a laser pulse, $\sigma_c = 1.1 (2.59) \cdot 10^{-25} cm^2$ is the total Compton cross section and S_{eff} is the effective area of the photon and electron beams intercept. Choosing $S_{eff} = 4 \cdot 10^{-6} cm^2$, one can easily get the laser energy per pulse

$$A_0 = n_0 \ \omega_0 \sim 19.2 \ (8.152) \ J,$$

corresponding to the total electron conversion. Since the optimal number of converted photons N_{γ} , defined by (4), is much less than N_e , we need not the total conversion of electrons and the required pulse energy is suppressed by the factor of K

$$A = K A_0 \sim 2.21 (2.88) \cdot 10^{-6} J$$

which is accessible with modern laser technology.

Finally we shall discuss a choice of the laser pulse frequency. It should evidently coincide with the linac frequency f_{pulse} when number of the bunches n_b

in the electron beam is equal to unity. If the electron beam has a multybunch structure, one may either choose the repetition rate of laser pulses to be equal to $f_{pulse} \cdot n_b$ or use a mirror system [11], which evidently decreases the laser pulse frequency. Since the detailed discussion of an experimental setup is beyond the scope of our paper, we choose for simplicity the laser pulse frequency equal to $f_{pulse} \cdot n_b$.

For the linear accelerators the integrated luminosity per a year of operation takes the form

$$L_{linac}^{int} = 10^7 \cdot f_{rep} \beta N_e K T_n,$$

$$f_{rep} = f_{pulse} \cdot n_b,$$
(6)

where f_{rep} is the collision frequency. Taking into account the Eq.(4), one can estimate L_{linac}^{int} as follows

$$L_{linac}^{int} = 10^7 \cdot \frac{f_{rep}}{\sigma_{\gamma p}} \sim 0.8 \ (0.012) \ fb^{-1}.$$
 (7)

2.2 Circular Accelerator

Now we briefly consider the possibility to obtain the real gamma beam at a circular electron accelerator, say at LEP2. All calculations are done in analogy with the TESLA case, except a few details. First of all, f_{rep} now takes the form

$$f_{rep} = f_{pulse} \cdot n_b = \frac{c}{2\pi R} \cdot n_b = 44 980 \ Hz,$$

where the number of electron bunches $n_b=4$, c is the speed of light, R is the ring radius and f_{pulse} is the circulation frequency in this case. It is evident that for the circular accelerator f_{rep} should coincide with frequency of the laser pulses. The next remark concerns the Eq.(5). We choose the effective area of the photon and electron beams intercept to be $S_{eff} \sim S_e = 2 \cdot 10^{-4} cm^2$, where S_e is the transverse area of the LEP2 electron beam, and the total Compton cross section $\sigma_c = 1.86 \cdot 10^{-25} cm^2$ at the LEP2 energy. And finally, we should take into account the effects of beam mean life time (we did not consider these effects earlier, since every electron bunch provided by the linear accelerator could be used only once).

In each collision about K N_e electrons are scattered. Since every bunch exercise the collision with the frequency $f_{pulse} = c/2\pi R \sim 1.12 \cdot 10^4 Hz$, the mean lifetime of the beam τ_b may be estimated as

Table 1 The parameters of the LEP2, SLAC and TESLA electron beams. Here f_{pulse} is the pulse frequency, H and V are the horizontal and vertical beam radius correspondingly, N_e is the number of electrons per bunch and n_b is the number of bunches.

8-57, 1 1 2			_			
	E_e (GeV)	$N_e (10^{10})$	n_b	$f_{pulse}(\mathrm{Hz})$	$H(\mu m)$	V (μm)
LEP2	100	40	4	$11.25 \cdot 10^3$	200	8
SLAC	50	3.5	1	120	2.1	0.6
TESLA	250	5.15	800	10	0.64	0.1

$$\tau_b = \frac{\log(1-\delta)}{\log(1-K)} \cdot \frac{1}{f_{pulse}} \sim 400 \ s,$$

where δ denotes the maximal fraction of electron loss permitted by beam dynamics. In what follows we choose $\delta = 0.1$, then the number of collisions each bunch exercises during one cycle, is equal to

$$l = \frac{\log(1 - \delta)}{\log(1 - K)} \sim 4.46 \cdot 10^6,$$

and the mean number of electrons in a bunch \hat{N}_e is given by

$$\hat{N}_e = (1 - \frac{l}{2}k)N_e,$$

where N_e denotes the initial number of electrons in a bunch.

For the ring accelerators the integrated luminosity per year of operation takes the form

$$L_{ring}^{int} = 10^7 \cdot \frac{\tau_b}{\tau_a + \tau_b + \tau_f} f_{rep} \beta \hat{N}_e K T_n,$$
(8)

where τ_a is an acceleration time, τ_f is a filling time. Taking into account the Eq.(4), one can estimate L_{ring}^{int} as follows

$$L_{ring}^{int} = 10^7 \cdot \frac{\tau_b}{\tau_a + \tau_b + \tau_f} f_{rep} \frac{\hat{N}_e}{N_e} \frac{1}{\sigma_{\gamma p}} \sim 0.27 fb^{-1}.$$
 (9)

Table 2

The real gamma beam parameters at LEP2, SLAC and TESLA. Here y_{max} is the ratio of the gamma beam maximal energy to the electron energy, θ_{γ} is the opening angle of the collimator, β denotes the fraction of photons coming through the slit, N_{γ} is the total number of converted photons, K is the conversion coefficient and A

is the laser energy per pulse.

		P					
	y_{max}	$ heta_{\gamma}$	β	N_{γ}	K	A	L^{int}
		$(10^{-6}rad)$		(10^4)	(10^{-7})	$(10^{-6}J)$	(fb^{-1})
LEP2	0.835	1.26	0.0265	0.945	0.236	13.4	0.27
SLAC	0.717	1.93	0.0202	1.236	3.53	2.88	0.012
TESLA	0.927	0.759	0.0422	0.592	1.15	2.21	0.8

The electron beam parameters, we have used in the estimations, are contained in Tabl. 1. while the γ -beam characteristics are given in Tabl. 2.

Thus the luminosity at a probable SLAC experiment is about one order of magnitude smaller compared with LEP2 case due to a lower collision frequency. Choosing a more powerful laser one can reach almost the same luminosity at SLAC, but the price will be too high: more than one hundred events per collision, which reduces significantly the range of the physical phenomena accessible for investigations. The luminosity at TESLA even exceeds the LEP2, since the TESLA project will operate with multybunch trains.

3 The Heavy Quark Photoproduction

The differential cross section of the photon-gluon fusion looks as follows [12]

$$\frac{d\hat{\sigma}}{d\hat{t}} = \frac{d\hat{\sigma}^n}{d\hat{t}} + \lambda_g \xi_2 \frac{d\delta\hat{\sigma}}{d\hat{t}},$$

where λ_g and ξ_2 denote the gluon and photon helicities. The spin averaged and polarized asymmetry distributions in the LO QCD take the form, corespondingly:

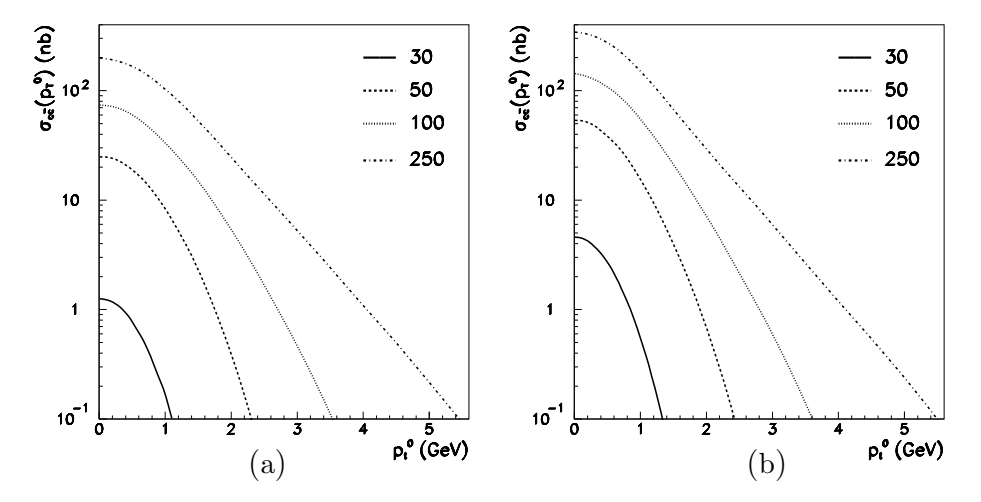


Fig. 1. The distribution of charm production $\sigma_{c\bar{c}}(p_t \geq p_t^0)$ versus p_t^0 for different electron energies: $E_e=30~GeV$ - solid line, $E_e=50~GeV$ - dashed line, $E_e=100~GeV$ - dotted curve, $E_e=250~GeV$ - dashed-dotted line. The c-quark mass is $m_c=1.5~GeV/c^2$ (a), $m_c=1.3~GeV/c^2$ (b).

$$\frac{d\hat{\sigma}^n}{d\hat{t}} = \frac{\pi\alpha\alpha_s(s)e_q^2}{\hat{s}^2} \left(\frac{4m^2\hat{s}}{(\hat{t}-m^2)(\hat{u}-m^2)} + \frac{\hat{u}-m^2}{\hat{t}-m^2} + \frac{\hat{t}-m^2}{\hat{u}-m^2} - \frac{4m^4\hat{s}^2}{(\hat{t}-m^2)^2(\hat{u}-m^2)^2} \right).$$
(10)

$$\frac{d\delta\hat{\sigma}}{d\hat{t}} = \frac{\pi\alpha\alpha_s(s)e_q^2}{2\,\hat{s}^2} \left(\left(\frac{\hat{u} - m^2}{\hat{t} - m^2} + \frac{\hat{t} - m^2}{\hat{u} - m^2} \right)^2 - \hat{s}(\hat{s} - 4\,m^2) \left(\frac{1}{(\hat{t} - m^2)^2} + + \frac{1}{(\hat{u} - m^2)^2} \right) \right), \tag{11}$$

Here $\hat{s}, \hat{t}, \hat{u}$ are the invariant variables of the subprocess, α , $\alpha_s(s)$ are the fine and strong coupling constants respectively and e_q denotes the c-quark charge.

The produced $c\bar{c}$ pairs can form J/ψ or fragment into D, D^* -mesons. In what follows we shall consider only the open charm production, because this process is more transparent from theoretical point of view. In addition, the open charm has an advantage over J/ψ production, because its cross-section is at least ten times larger for attainable photon energies.

The accumulated p_t -distribution of charmed quarks

$$\sigma_{c\bar{c}}(p_t^0) = \int_{p_t \ge p_t^0} dp_t \int \frac{d\hat{s}}{s} \frac{d\hat{\sigma}^n}{dp_t} G(x, Q^2)$$
(12)

versus p_t^0 is shown in Fig.1, and Fig. 2 presents the same dependence for

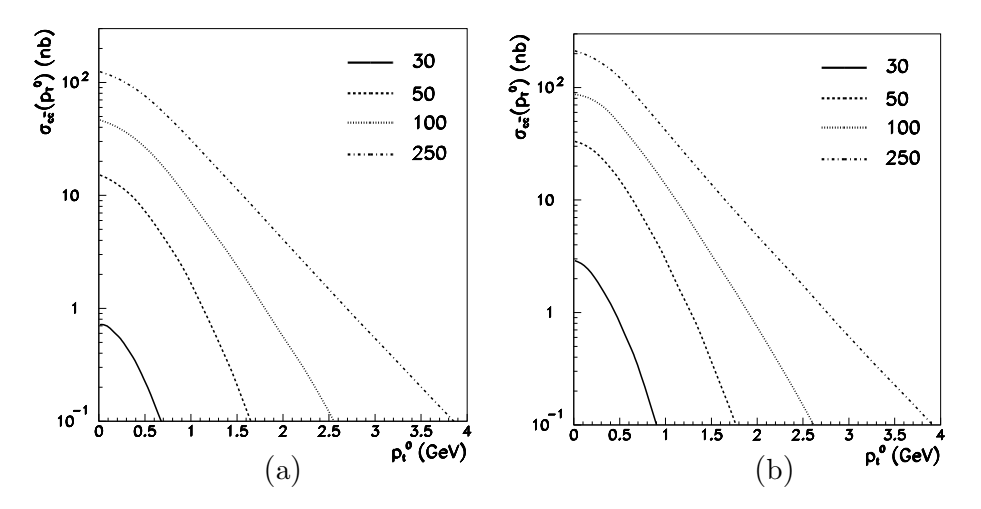


Fig. 2. The distribution of the inclusive D^* -meson production $\sigma_{D^*} \chi(p_t \geq p_t^0)$ versus p_t^0 for different electron energies: $E_e = 30~GeV$ - solid line, $E_e = 50~GeV$ - dashed line, $E_e = 100~GeV$ - dotted curve, $E_e = 250~GeV$ - dashed-dotted line. The c-quark mass is $m_c = 1.5~GeV/c^2$ (a), $m_c = 1.3~GeV/c^2$ (b).

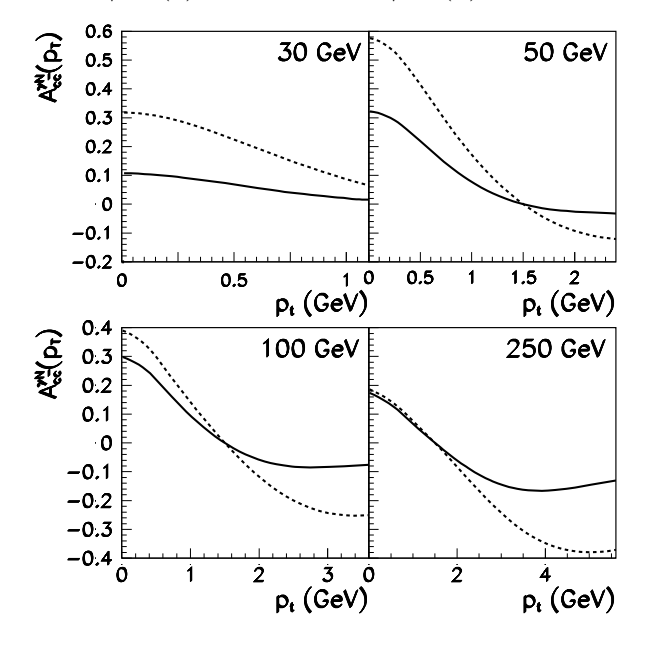


Fig. 3. The differential asymmetry $A_{c\bar{c}}^{\gamma N}(p_t)$ of the c-quark production versus p_t for the c-quark mass equal to 1.5 GeV/c^2 . The solid (dashed) line corresponds to the set A (B) of polarized gluon density [9].

inclusive D^* -meson production

$$\sigma_{D^*}(p_t^0) = \sigma_{D^{*+}}(p_t^0) + \sigma_{D^{*0}}(p_t^0).$$

In our estimates we have used the parametrizations of both polarized and unpolarized gluon densities from [13], c-quark fragmentation functions were taken from [14], α_s from the global analysis of DIS data [15]. A gamma beam

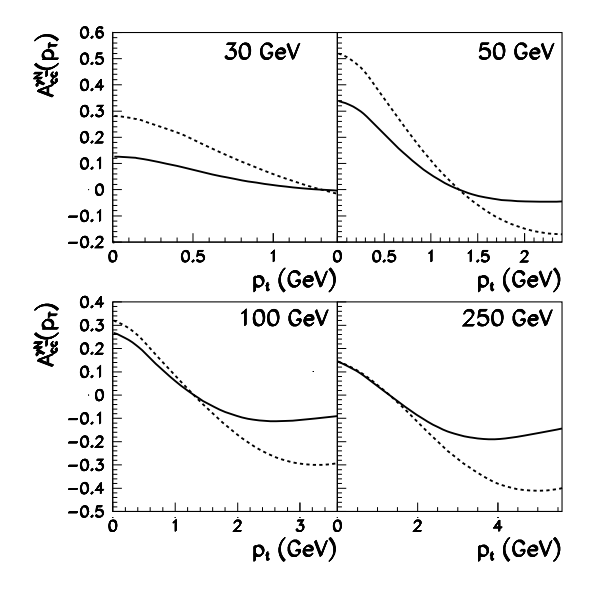


Fig. 4. The differential asymmetry $A_{c\bar{c}}^{\gamma N}(p_t)$ of the c-quark production versus p_t for the c-quark mass equal to 1.3 GeV/c^2 . The solid (dashed) line corresponds to the set A (B) of polarized gluon density [9].

spectrum was chosen as monochromatic with energy $E_{\gamma} = \kappa/(1+\kappa)E_e$ for $E_e \geq 50~GeV$, while for $E_e = 30~GeV$ the smeared-out spectrum, given by (2), was used. Numerical integration was performed with the help of adaptive integration code [16]. All distributions have similar form and decrease exponentially with p_t^0 rise when transverse momentum exceeds 1~GeV/c. One concludes that the estimated production rate of D^* -mesons with large transverse momentum $p_t \geq 1~GeV/c$ is sizeable and reaches approximately 30 nb (40 nb) at TESLA energy for c-quark mass equal to 1.5 (1.3) GeV/c^2 correspondingly.

The differential asymmetry $A_{c\bar{c}}^{\gamma N}(p_t)$ of c-quark production versus p_t

$$A_{c\bar{c}}^{\gamma N}(p_t) = \frac{d\delta\sigma}{dp_t} / \frac{d\sigma^n}{dp_t}$$
(13)

is shown in Figs. 3–4 for the c-quark mass 1.5 (1.3) GeV/c^2 correspondingly, and analogous dependences for D^* -meson production are pictured in Figs. 5–6 for the same mass set. Here we have introduced the following notations

$$\frac{d\sigma^n}{dp_t} = \int \frac{d\hat{s}}{s} \frac{d\hat{\sigma}^n}{dp_t} G(x, Q^2),$$

$$\frac{d\delta\sigma}{dp_t} = \int \frac{d\hat{s}}{s} \frac{d\delta\hat{\sigma}}{dp_t} \Delta G(x, Q^2).$$

As is already known, the differential asymmetry of $c\bar{c}$ production, derived in

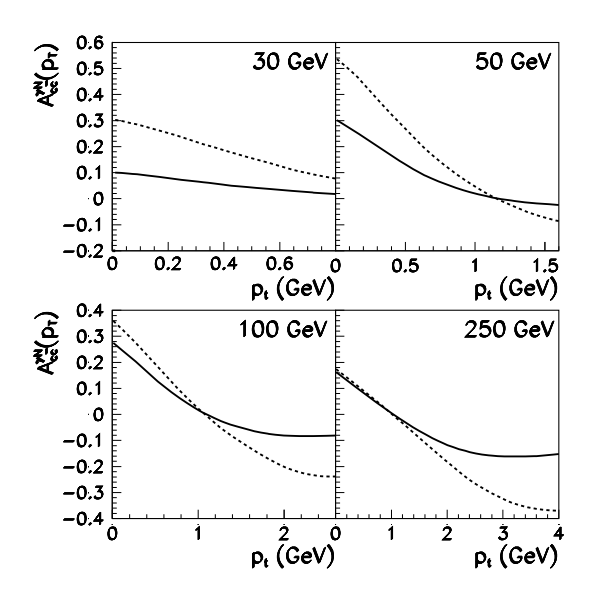


Fig. 5. The differential asymmetry $A_{D^*}^{\gamma N}(p_t)$ of the D^* meson production versus p_t for the c-quark mass equal to 1.5 GeV/c^2 . The solid (dashed) line corresponds to the set A (B) of polarized gluon density [9].

the LO approximation, has a kinematic zero at $p_t = m_c$ and then changes a sign. For D^* -meson production a zero position shifts to the lower value of $p_t \sim 1~GeV/c$ due to fragmentation smearing. Integration over total range of p_t evidently decreases the asymmetry, so it is reasonable to introduce a kinematic cut on the D^* -meson transverse momentum, say $p_t \geq 1~GeV/c$. In this region $A_{D^*}^{\gamma N}(p_t)$ does not change sign, moreover the predicted asymmetry value heavily depends on the choice of polarized gluon distribution. It is due to the fact that the main contribution to production of D^* - mesons having large transverse momentum comes from the region $x \geq 0.1$, where $\Delta G(x, Q^2)$ is poorely known. At present there are plausible restrictions on the polarized gluon density only at $x \leq 0.1$, where all model predictions almost coincide. Then the precise measurement of polarized gluon density at $x \geq 0.1$ will surely help to choose a reasonable parametrization of $\Delta G(x, Q^2)$.

Let us briefly discuss the next-to-leading (NLO) corrections to the charm production process. As it was shown in [17], these corrections are quite sizeable at SLAC and CERN experiments, so one should introduce large K-factor to take into account NLO corrections. It is not the case at TESLA, where NLO correction to the total asymmetry does not exceed 0.3-0.5. Then one may hope that higher order corrections will also be under control at possible TESLA experiment. It is not improbable, because all invariants (taking into account introduced kinematic cut) are sufficiently large at TESLA energy. The total asymmetry is of the order 10 % at $\sqrt{s_{\gamma p}} \sim 10~GeV$ and decreases with energy rise to a few percent when $\sqrt{s_{\gamma p}} \sim 20~GeV$ [17]. The introduced kinematic cut on D^* –meson transverse momentum surely rises this value, because the differential asymmetry $A_{D^*}^{\gamma N}(p_t)$ does not change sign beyond $p_t \sim 1~GeV/c$.

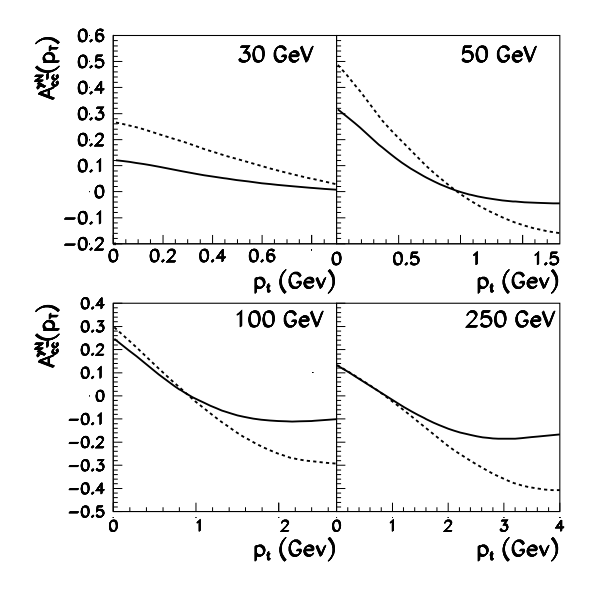


Fig. 6. The differential asymmetry $A_{D^*}^{\gamma N}(p_t)$ of the D^* meson production versus p_t for the c-quark mass equal to 1.3 GeV/c^2 . The solid (dashed) line corresponds to the set A (B) of polarized gluon density [9].

4 Event Reconstruction

4.1 D^* - tagging

One of the best method for D^* - tagging uses the kinematic constraint of the decay chain:

$$D^* \to D\pi \to (K\pi)\pi. \tag{14}$$

The difference of the invariant masses

$$\Delta M = m(K\pi\pi) - m(K\pi) = m(D^*) - m(D) \sim 145 \ MeV/c^2$$
 (15)

is very close to the π -meson mass, and can be determined with precision about 2.5 MeV/c^2 [6], significantly exceeding accuracy of D^* -meson mass measurement. It permits to reduce substantially the background to D^{*+} -meson production, for example, COMPASS estimates showed that the background is less than 10 %.

The isospin invariance suggests equal D^{*+} and D^{*0} production rates, then $\sigma(D^{*+} X) \sim 0.5 \cdot \sigma(D^* X)$. Since the branching ratio for the decay chain (14) is 2.6 %, about $\sim 62.4 \cdot 10^4$ (83.2 · 10⁴) D^{*+} -mesons with p_t exceeding 1 GeV/c will be produced at TESLA energy in a year. Assuming an overall acceptance to be equal to 0.2 [6], we expect to reach a reconstruction rate of

Table 3 The target parameters. Here P_t is the target polarization, f_t denotes the fraction of the polarized target nucleons, T_n stands for the target density, and L is the target length.

	f_t	P_t	$T_n (10^{25} cm^{-2})$	L(cm)
butanol	0.24	0.8	4	40

$$N_{D^{*+}} = 124.8 \cdot 10^3 \ (166.4 \cdot 10^3) \cdot year^{-1}. \tag{16}$$

A rigorous evaluation of acceptance will change these figures, because COM-PASS experiment uses kinematic cuts different from ours. Nevertheless, the equality (16) gives a good idea about the actual reconstruction rate, attainable in the proposed experiment.

The observed spin asymmetry $A_{D^*}^{exp}$ of D^{*+} -meson photoproduction with account of the beam and target polarizations is given by

$$A_{D^*}^{exp} = P_b P_t f_t A_{D^*}^{\gamma N}. (17)$$

Here the asymmetry $A_{D^*}^{\gamma N}$ is the ratio of helicity dependent and helicity averaged cross sections for D^{*+} -meson production in γN -collisions, calculated with account of kinematic cuts. Parameters P_b , P_t are the beam and target polarizations, f_t denotes the fraction of the polarized target nucleons. The target characteristics are given in Tabl. 3, while the gamma beam polarization P_b is about unity.

We impose the p_t cut on D^* -meson transverse momentum and choose three values of p_t : 0, 1, 2 GeV/c. The statistical precision of $A_{D^*}^{\gamma N}$ with account of target properties is given by

$$\Delta A_{D^{*+}}^{\gamma N} \sim \frac{1}{\sqrt{N_{D^{*+}}} f_t P_b P_t} = 2.08 (1.81) \cdot 10^{-2},$$
 (18)

for the cut $p_t \geq 1~GeV/c$. One can achieve even better statistical precision by detecting D^* mesons in the total kinematic region of p_t (Tabl.4). On the other hand, "strong" cut on the transverse momentum, say $p_t \geq 2~GeV/c$, will lower the statistical accuracy by a factor of three, because the corresponding cross section does not exceed 3–4 nb. Our opinion is that the "moderate" restriction $p_t \geq 1~GeV/c$ is best suited for investigation of gluon polarization. Under this cut the total cross section is still sizeable, which results in a reasonable value

Table 4 The registration rates of D^{*+} mesons at TESLA. Here σ is the cross section of inclusive D^* meson production, $N_{D^{*+}}$ denotes the total number of observed D^{*+} mesons per year with account of efficiency, $\Delta A_{D^{*+}}^{\gamma N}$ stands for the statistical precision.

	$\sigma(nb)$	$N_{D^{*+}}(10^3)$	$\Delta A_{D^{*+}}^{\gamma N}(10^{-2})$
$p_t \ge 0$	126 (215)	524.2 (894.4)	0.72 (0.55)
$p_t \ge 1 \; GeV/c$	30 (40)	124.8 (166.4)	1.47 (1.28)
$p_t \ge 2 \; GeV/c$	4.1 (5)	17.1 (20.8)	3.99 (3.61)

of statistical precision, moreover it permits to decrease background and reduce uncertainties in the c-quark fragmentation process.

4.2 D^0 tagging

Experimentally, total number of D^0 -mesons per charm event is approximately equal to the sum of D^{*+} - and D^{*0} -meson production rates. Produced D^0 may be detected via the simplest two - body decay

$$D^0 \to K^- \pi^+,$$

with the branching ratio of 3.8%. An estimate shows that D^0 - meson reconstruction rate is more than corresponding quantity for D^{*+} -meson by a factor of three due to a larger value of both the D^0 -production cross section and decay branching ratio. However, unlike the D^{*+} -tagging, a background to the D^0 -production remains significant even after account of kinematic cuts, and it exceeds signal, for example at COMPASS, by a factor of four [6]. It means that correct evaluation of both the asymmetry and statistical precision of measurement requires a detailed analysis of the background, which is beyond the scope of our paper.

4.3 Single muon tagging

The most simple method to select charm production events consists in the detecting of muons from semileptonic D-meson decays. Muons coming from light meson decays, as well as Bethe-Heitler pairs, contribute mainly to the low values of p_t , so one may reduce these backgrounds by imposing cut on D-meson transverse momentum, say $p_t \geq 1 \ GeV/c$. Assuming the branching

ratio of the decay

$$D^{0\,(+)} \to \mu + X,$$

to be 6.8 % for D^0 and 17.2 % for D^+ -meson, and ratio of the D-meson production rates per charm event to be

$$\frac{N_{D^0}}{N_{D^+}} \sim 3,$$

one expect about $N_{\mu}=4.51~(6.02)\cdot 10^6$ prompt muons at TESLA for $m_c=1.5,~(1.3)~GeV/c^2$ correspondingly. In average, muon acquires a transverse momentum equal to about one half of the parent meson mass, that is 1~GeV/c in our case. To obtain a rough estimate, suppose that only one half of muons coming from decays of D-mesons with $p_t\geq 1~GeV/c$ will get a transverse momentum larger than 2~GeV/c. In this case a reconstruction rate is given by

$$N_{\mu} \sim 2.26 \ (3.01) \cdot 10^6$$

under assumption of 100 % muon detection efficiency. The precision of the asymmetry measurement with account of the target properties can be roughly estimated as

$$\Delta A_D^{\gamma N} \sim \frac{1}{\sqrt{N_\mu} f_t P_b P_t} = 3.5 (3.0) \cdot 10^{-3}.$$
 (19)

The exact evaluation of the statistical error requires a close investigation of the background. Nevertheless Eq. (19) gives a good idea about an actual precision one may hope to reach at TESLA experiment. We remind, for comparison, that SLAC collaboration expected to obtain statistical accuracy of asymmetry measurement about $6 \cdot 10^{-3}$ under severe conditions of large background coming from pile up of the events.

5 Conclusion

In the present paper we have considered an opportunity to use polarized real photon beam for investigation of polarized gluon distributions. Our estimate back up the possibility to achieve a higher accuracy in the measurement of charm photoproduction asymmetry compared with planned experiments at SLAC and CERN. The proposed experiment may give unambiguous information about both the total value and the x- dependence of gluon polarization,

which will permit to reduce significantly the number of acceptable models decsribing nucleon spin effects.

References

- J. Ashman et al, Phys. Lett. **B206** (1988), 364;
 Nucl. Phys. **B328** (1989) 1.
- [2] J. Ellis and R. Jaffe, Phys. Rev. **D9** (1974) 1444;Phys. Rev. **D10** (1974) 1664 (E).
- [3] A. Efremov and O. Teryaev, JINR-E2-88-287 and Phys. Lett. **B240** (1990) 200;
 G. Altarelli and G. Ross, Phys. Lett. **B212** (1988) 391.
- [4] R. L. Jaffe, Phys. Lett. **B365** (1996) 359.
- [5] J.J. Aubert et al, Phys. Lett. **B110** (1982) 73.
- [6] COMPASS Proposal, CERN/SPSLC 96-14, SPSC/P 297.
- S. Alekhin, V. Borodulin and S. Sultansoy, Int.J.Mod. Phys. A8 (1993) 1603;
 S. Atag et.al., Europhys. Lett. 29 (1995) 815; Nucl. Instr. and Meth. A381 (1996) 23;
 - V. Borodulin et al., Proceedings of the 2^{nd} spin workshop, Zeuthen, 1997. Eds.: J.Blumlein, A.DeRoeck, T.Gehrmann and W.D.Nowak. p. 439; M.Duren, the same proceedings, p. 414.
- [8] Conceptual Design of a 500 GeV e+e- Linear Collider with Integrated X-ray Laser Facility, Eds: R.Brinkmann. G.Materlik, J.Rossbach, A.Wagner, DESY 1997-048, ECFA 1997-182.
- [9] I. F. Ginzburg et al., Nucl. Instr. and Meth. **205** (1983) 477.
- [10] S. Atag et al., Nucl. Instr. and Meth. **A381** (1996) 21.
- [11] Ciftci et.al., NIM **A365** (1995) 317.
- [12] G. Altarelli and W.J. Stirling, Particle World 1 (1989) 40;
 W. Vogelsang, in Physics at HERA, Vol. 1, eds. W. Buchmuller and G. Ingelman, (1991) 389.
- [13] T. Gehrmann and W.J. Stirling, DTP/95/82, hep-ph/9512406.
- [14] C. Peterson et al., Phys. Rev. **D27** (1983) 105.
- [15] S.I. Alekhin, IHEP 96-79, hep-ph/9611293, 1996, to appear in Eur. Phys. Jour.
- [16] T.A. Merkulova and G.G. Takhtamyshev, JINR-E11-95-255, 1995.
- [17] I. Bojak and M. Stratmann, DTP/98/22, hep-ph/9804353;
 I. Bojak and M. Stratmann, DTP/98/36, hep-ph/9807405.